Size Effect in Strength Assessment by Indentation Testing on Rock Fragments

M. Haftani[a 1], B. Bohloli[a], A. Nouri[b], M.R. Maleki Javan[a], M. Moosavi[c]

[a] School of Geology, College of Science, University of Tehran, Iran

[b] Department of Civil and Environmental Engineering, University of Alberta, Canada

[c] School of Mining Engineering, College of Engineering, University of Tehran, Iran

Abstract

In this study, uniaxial compressive strength (UCS) of limestone rocks was estimated by indentation testing on small rock fragments. Here, the effects of rock fragment dimensions (particularly area and thickness) on indentation indices were studied. The investigation shows size dependency of the conventional indentation parameters. The results indicate the fragment area normal to loading direction has little effect on the indentation indices, while the sample thickness has major influence on the results. To reduce size dependency, the results of indentation test were normalized by a thickness function.

The proposed empirical equations were verified against independent data pertaining to other limestone rocks not used in developing the correlations, which showed agreement between the estimated and measured UCS. Statistical analysis was used to determine the minimum number of required indentation tests in relation to the project importance. This study shows that the uniaxial compressive strength of rocks can be estimated reasonably well from indentation testing of small rock fragments.

Key words: *Indentation Test, Drill Cutting, Size Dependency, Normalized Indentation Stiffness, Normalized Critical Transition Force, Uniaxial Compressive Strength, Geomechanical Characterization.*

1. Introduction

Uniaxial compressive strength (UCS) of rocks is widely used as a strength index parameter for rock mass classification [1,2] and studies related to underground mining [3], slope stability [4,5], oil well drilling [6,7], wellbore stability [8-10] and sand production [11]. Laboratory testing on rock cores [12,13] and acoustic well logging [14,15] are two well-known techniques to assess mechanical properties of rocks (including the UCS). Even though these methods result in reliable assessment of the intact rock strength, expensive coring and logging operations restrict their use to only important intervals.

Several indirect and unconventional techniques and procedures have been established to obtain formation mechanical properties. These include correlations between the desired

[1] **Corresponding Author:**
Mohammad Haftani, (E-mail Address: m.haftani@khayam.ut.ac.ir)
(M. Haftani: Currently visiting Researcher at the University of Alberta; Tel.: +1 587 710 9356)
Postal Address: Department of Structural and Engineering Geology, School of Geology, College of Science, University of Tehran, Enghelab Ave., Tehran, Iran (**Tel. & Fax:** +98 21 66 49 16 23)

properties and easily and reliably measured parameters [16,17] and mineralogical and textural characteristics [18-20]. In addition, although drill cuttings have not generally been used as a source for rock property evaluation, vast laboratory studies have been carried out to investigate their potential in formation evaluation. Santarelli et al. [21] stated that drill cuttings can be used as representative of the formation materials and a reliable source of information about their mechanical and physical properties. Subsequently, many testing approaches have been developed to utilize small rock fragments (drill cuttings) for determination of the uniaxial compressive strength. Measuring P and S wave velocities by pulsed ultrasonic on cuttings and continuous wave technique [21, 22], reconstructed core samples [23] and indentation testing [e.g. 7,15,21,24,25] are a few such approaches to mention.

Using indentation testing, Zausa and Santarelli [25] developed a power correlation between the indentation stiffness and UCS. Szwedzicki [26] showed the potential of indentation testing in estimation of mechanical properties of rock by a relationship between the values of the Indentation Hardens Index (as the maximum load divided by the maximum penetration) and UCS. Uboldi et al. [6] found that the indentation test provides an index value directly related to the rock UCS. Many researchers attempted to develop practical correlations between the indentation indices and the UCS for sandstones, limestones and shales with different strengths and deformation characteristics [e.g. 6,7,15,21,24].

Ringstad et al. [24] showed high dependency of indentation parameters to sample sizes. Also, Zausa and Santarelli [25] found size dependency for high-porosity rocks, and low sensitivity to size for low-porosity rocks.

In majority of these studies, indentation test has been performed on samples with random dimensions of 2-5 mm or larger even up to 50 mm. Thus, contrary to previous works where the fragment size effect was not quantified rigorously, we provide a statistical correlation of UCS against normalized indentation indices (IS_n and CTF_n) in which effect of the thickness of specimen is considered. This study employs fragments with certain shape and sizes to study the size effect.

2. Experimental Study

2.1 Sample preparation and testing procedure

Rock samples used in this study include nine limestone blocks (S1-S9) with strengths ranging from 30 MPa to 280 MPa collected from different locations throughout Iran. Based

on the Folk's classification, the limestone blocks can be classified as micritic limestone formed of homogeneous calcareous particles ranging in diameter up to 4 μm [27]. Physical and mechanical properties were determined using standard laboratory methods on intact rock samples (see Table 1).

Table 1: Physical and mechanical characteristics of the samples.

Sample No.	Lithology	Rock Density (g/cm^3)	Porosity (%)	UCS (MPa)
S1	Micritic Limestone	2.59	2.25	279.76
S2	Micritic Limestone	2.64	2.62	230.39
S3	Micritic Limestone	2.73	< 0.10	182.49
S4	Siliceous Limestone	2.65	0.91	129.73
S5	Siliceous Limestone	2.64	0.93	124.39
S6	Marly Limestone	2.43	9.64	31.50
S7	Micritic Limestone	2.72	1.16	246.32
S8	Micritic Limestone	2.63	6.06	178.45
S9	Siliceous Limestone	2.64	1.07	82.89

Note: Blocks S1 to S6 were utilized to evaluate the indentation test results and blocks S7 to S9 were used to verify the accuracy of the proposed equations.

The rock samples were cut into rectangular cuboids with the dimensions of 3×3, 4×4 and 5×5 mm^2 and the thickness of 1, 2 and 3 mm. To avoid damage of rock fragments during preparation samples were first cut by a diamond saw machine and then grinded at the faces. The artificial rock fragments were embedded in a disk shaped epoxy-resin of 55 mm in diameter and 10 mm thickness (Fig. 1a). The reasons for using epoxy-resin were to: a) contain the fragments during testing, and b) generate a smooth surface of rock fragment for normal loading. The epoxy-resin had epoxy aliphatic structure made of two components of resin epoxy bisphenol and polyamine hardener. After curing of resin, a disk was trimmed and polished to expose the face of rock fragments for indentation testing. For each of the samples, a total of 90 rock fragments were placed in nine epoxy-resin disks each including 10 samples of the same size (e.g. disk S1-T3-A5×5 included 10 rock fragments of limestone S1 with thickness of 3 mm and area of 5×5 mm^2, as shown in Fig. 1a).

In this study, a cylindrical flat-end indenter stylus with the diameter of 1 mm was used for applying load on rock fragments (Figs. 1b and 1c). The indenter was made of tungsten

carbide with ASTM hardness of 91 Rockwell B. A constant penetration rate of 0.01 mm/s was applied normal to the center of the rock fragment in agreement with the procedure described in Garcia et al. [7] and Mateus et al. [15] until load-penetration curve shows softening behavior. The applied force and penetration rate were measured during testing with load cell and displacement sensor, respectively (Fig. 1c). Data of fragments from limestone blocks S1 to S6 were used to develop correlation equation and those of blocks S7, S8 and S9 were utilized to verify the correlations. It should be mentioned that the samples were of fine grain micritic limestones and the grain size was negligible comparing to the size of the indenter of 1 mm. In the case of coarse grain samples, this size of indenter might have caused some errors.

2.2 Description of the measured parameters

Indentation testing includes measurement of force and displacement of an indenter which penetrates into a rock fragment until it breaks apart. Test data are presented in the form of load (N) versus penetration (mm), as shown in Fig. 1d. Conventionally, two main indices are derived from the indentation curve; Indentation Stiffness (IS) and Critical Transition Force (CTF), (see Fig. 1d):

- Indentation stiffness is defined as the slope of the linear part of the curve and is a measure of the rock resistance against the indenter penetration. In the literature, different terms were used to introduce the slope of the linear part of the curve; e.g. Indentation Index [6], Indentation Modulus [7, 15, 24], Indentation Number [21, 25] and Indentation Hardness Index [26].
- The critical transition force is the magnitude of load at the onset of softening.

The required number of fragments for testing was determined based on the small-sampling theory recommended by Gill et al. [28] through the following equations:

$$CV_{ob} = \frac{s}{\overline{X}} \times 100 \qquad (1)$$

$$N = \left[\left(\frac{p+1}{p-1} \right) t\beta \frac{CV\,ob}{100} \right]^2 + 1 \qquad (2)$$

where, CV_{ob} is the calculated coefficient of variation after testing, s is the standard deviation, $\overline{X}$ is the arithmetic average value, t_β represents the confidence coefficients which is obtained from the Student t distribution as a function of the number of degrees of freedom (N-1) and p is the reasonable precision index depending on the investigation importance.

In this study, p value of ≤1.20 was considered consistent with the guidelines of Gill et al. [28] for research work.

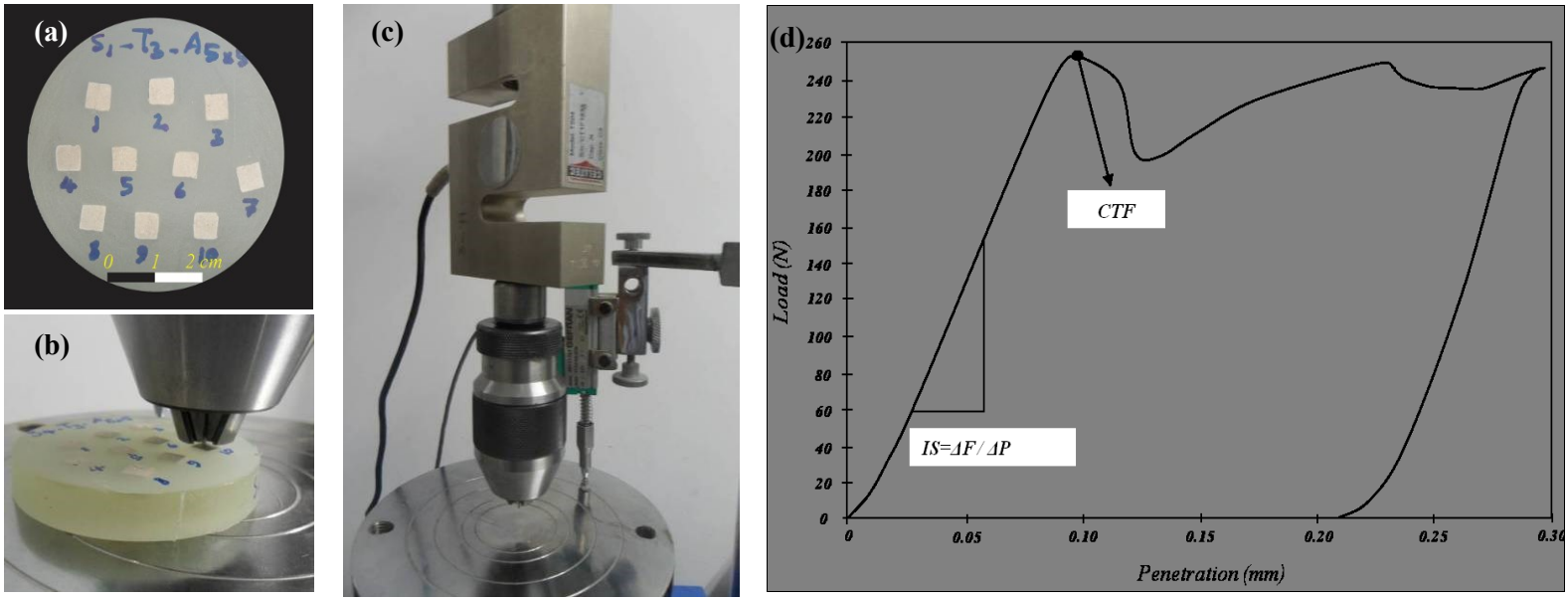

Fig. 1: a) Sample preparation by embedding the artificial rock cuttings in epoxy; each sample has 10 rock fragments with the same area and thickness (sample S1-T3-A5×5), b) cylindrical flat-end indenter stylus loads normal to the rock fragments, c) indentation equipment used in this study and d) typical load-displacement curve measured during the indentation test [7], Indentation Stiffness (IS) and Critical Transition Force (CTF) are illustrated on the curve.

3. Results and Discussions

3.1 Test results

A total of 540 indentation tests were carried out on rock fragments of limestone embedded in disk shaped epoxy-resin (90 fragments for each block S1,...,S6). Macroscopic and microscopic residual imprints of the indenter and post failure fractures are presented in Fig. 2.

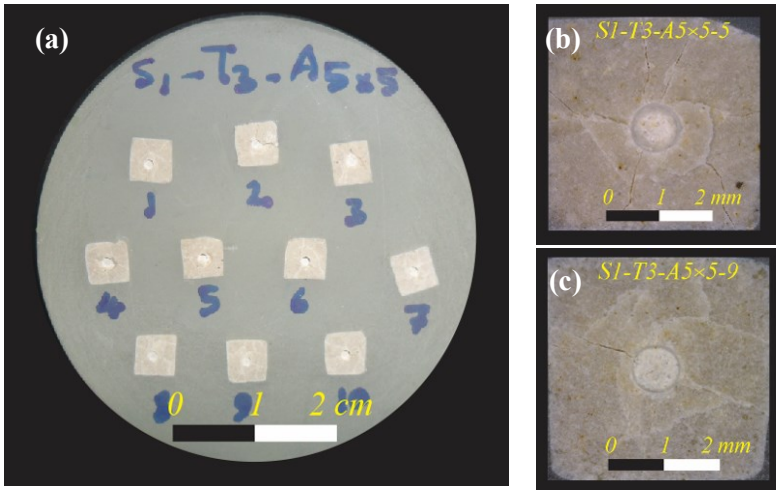

Fig. 2: Residual imprint of indenter after indentation test on sample S1-T3-A5×5, a) macroscopic photo, b and c) close-up of the failed fragments (magnification ×50).

Average value of the conventional indentation stiffness (IS) and critical transition force (CTF) were determined from the load-penetration curves recorded during the test (Table 2). In addition, the relevant coefficients of variations were calculated for each specimen group in a disk to determine the dispersion of the indentation parameters and the minimum number of test required (Fig. 3). The results are discussed in the following sections and are briefly summarized as:

- Coefficient of variation of the indentation stiffness (7.35%) was less than that of the critical transition force (9.13%). Thus, using Eq. (2) and considering $p \leq 1.2$ as a reliable precision index in the research work, 10 indentation tests are required for a 95% confidence interval when testing uniform-size samples.
- Area of the samples had no meaningful effect on the indentation indices, but the sample thickness affects the results significantly (see Section 3.2).
- The value of the indentation indices increases for thicker samples and varies with rock strength (see Section 3.2), which necessitates normalizing the conventional indentation indices (see Section 3.3).

Table 2: Results of the indentation test on the modified rock samples with different sample thicknesses (1, 2 and 3 mm) and areas (3×3, 4×4 and 5×5 mm^2).

Sample No.	Thickness= 1mm			Thickness= 2mm			Thickness= 3mm		
	Rock Fragment Area (mm × mm)								
	3×3	4×4	5×5	3×3	4×4	5×5	3×3	4×4	5×5
	Critical Transition Force (N)								
S1	386.45	373.27	366.33	739.52	683.67	731.37	1073.86	1075.39	1090.71
S2	403.03	409.23	396.54	689.09	687.78	696.08	1027.61	1056.96	1106.55
S3	331.65	307.19	306.85	757.33	769.51	785.25	1117.89	1238.99	1232.74
S4	374.51	367.22	390.18	794.71	777.51	824.58	1022.48	1096.86	1186.52
S5	427.53	446.30	440.11	890.48	829.26	909.58	1130.76	1332.05	1410.34
S6	221.93	264.07	251.24	315.77	264.72	292.59	318.68	312.25	333.22
	Indentation Stiffness (N/mm)								
S1	2990.85	2925.78	2932.60	3672.57	3206.17	3375.86	3855.30	3780.13	3979.98
S2	2952.25	2931.58	2884.90	3989.29	3901.07	4093.17	4686.01	4552.83	4496.30
S3	2417.95	2453.27	2364.36	3372.14	3613.56	3339.31	4032.86	4072.38	4230.30
S4	2663.77	2593.00	2783.71	3328.01	3226.84	3394.54	3800.97	3665.71	3730.63
S5	2789.64	2734.59	2887.06	3577.24	3580.26	3315.99	3972.61	3650.57	3842.93
S6	1444.35	1804.14	1594.20	2573.72	2765.96	2735.70	3184.94	2841.18	2986.40

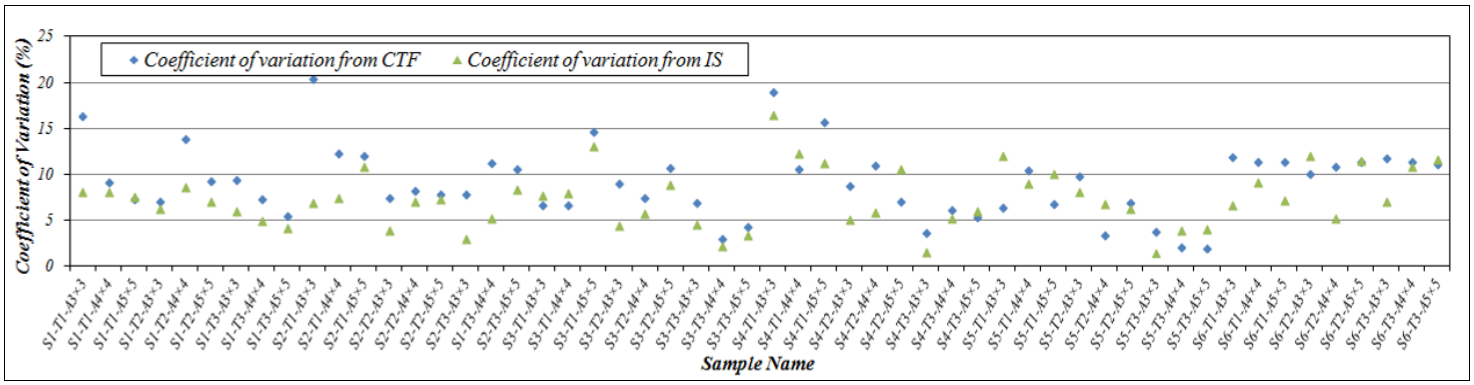

Fig. 3: Average value of calculated coefficient of variations for each specimen group in a disk after test.

3.2 Sample size effect

Experimental indentation test results were used to investigate the effect of fragment dimensions (thickness and area) on the indentation indices (Table 2).

Fig. 4 shows the effect of sample dimension on the variation of the indentation indices. This figure shows that samples with different areas have approximately the same indentation indices. On the contrary, indentation indices are sensitive to the sample thickness; the thicker the sample, the higher are the indentation indices.

Fig. 5 shows the data points pertaining to the indentation indices against the UCS of the corresponding intact rocks. Exponential regression curves were developed for the samples with the same dimensions which result in correlation coefficients greater than 0.60. In Fig. 5, correlation curves of the samples with different cross sectional areas nearly match, unlike the curves belonging to samples with different thicknesses. These correlation curves confirm the dependency of the indentation results on fragment thickness but low sensitivity to the cross sectional area normal to the loading direction. Additionally, the curves show diverging trends, indicating higher size dependency for stronger rock samples.

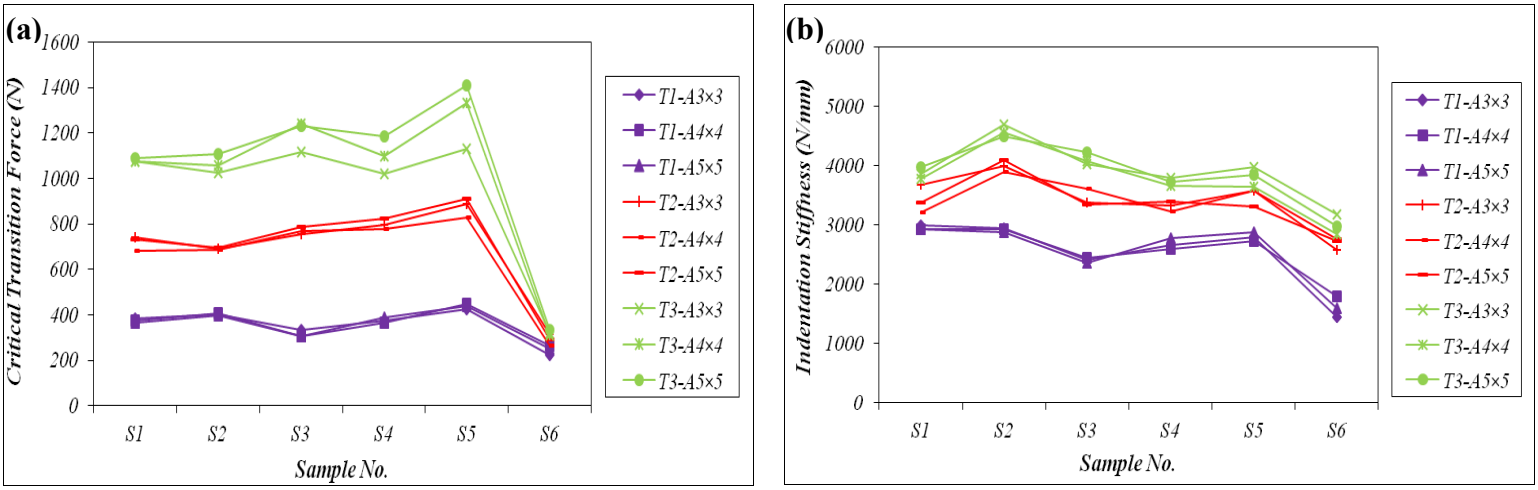

Fig. 4: a) Variation of critical transition force with sample size and b) variation of indentation stiffness with sample size.

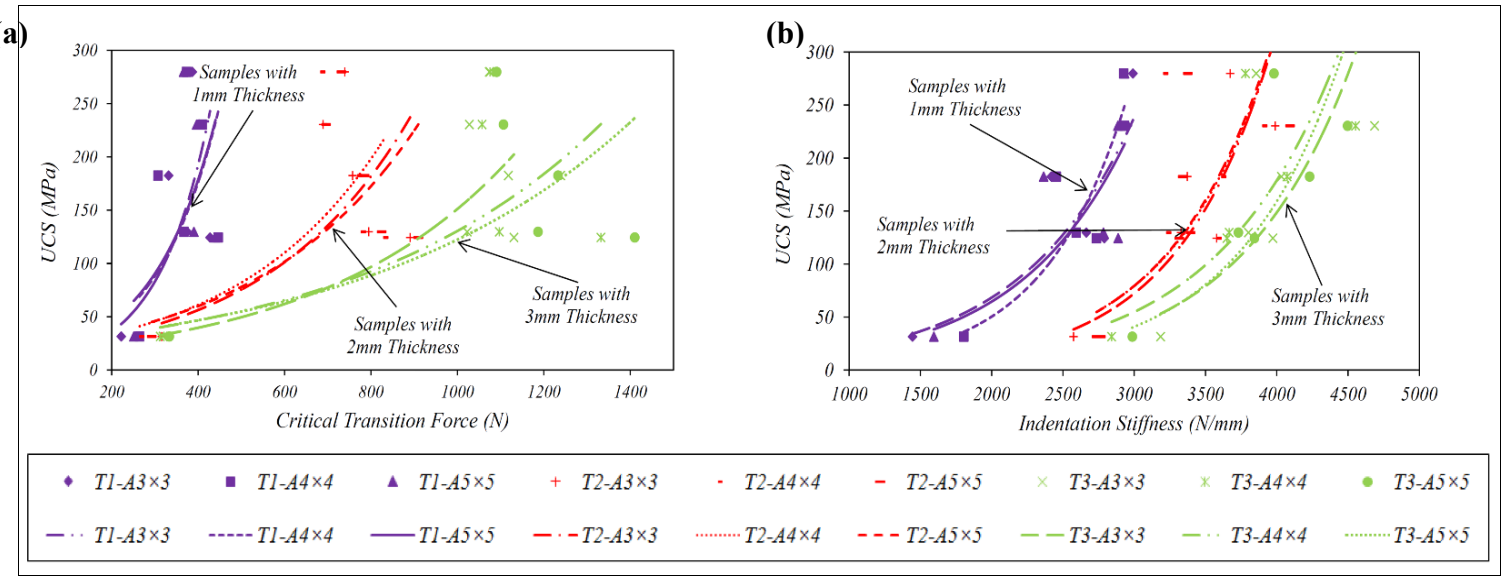

Fig. 5: Correlation between the indentation indices and the corresponding UCS, a) critical transition force and b) indentation stiffness. Each curve is obtained from the data of indentation testing on the fragments with the same dimensions. (Legend is same in both a and b which is presented below the curves).

3.3 Experimental correlation

This study showed that the thickness of rock fragments affects results of indentation testing. To reduce this dependency, we propose normalizing the indentation indices by a parameter that is function of the sample thickness and strength.

To demonstrate the degree of thickness effect on the indentation indices, IS and CTF of fragments were plotted versus the corresponding thickness (Fig. 6). The figure indicates higher indentation indices for thicker samples. Furthermore, it shows that rock strength affects slope of the correlation curves in power regression type, particularly for the critical transition force.

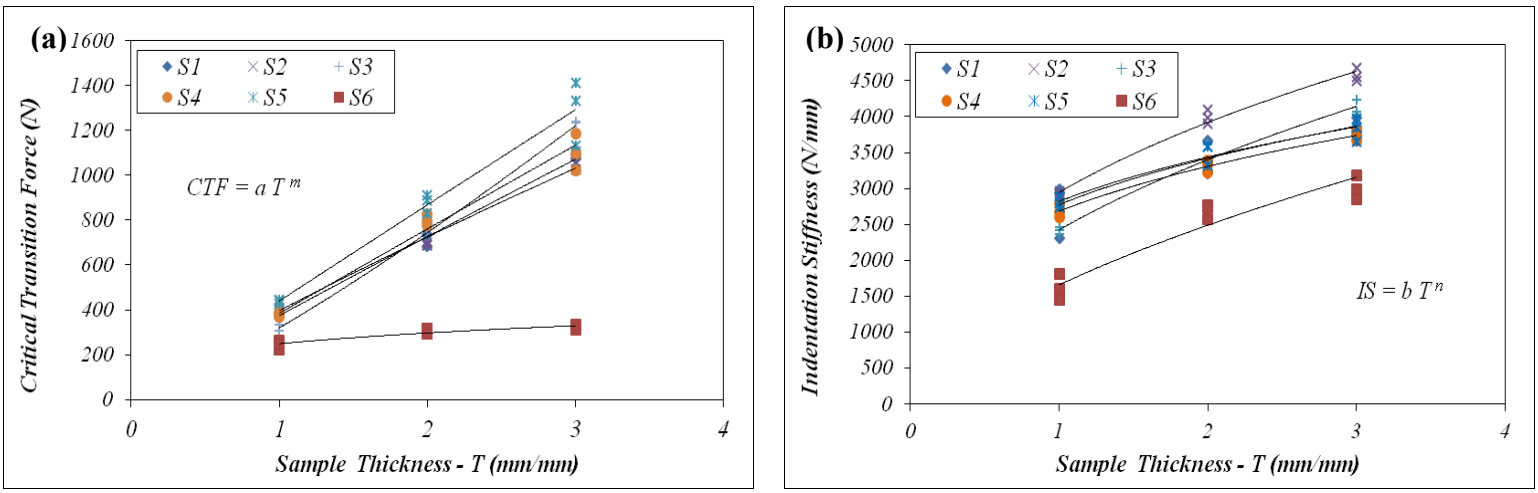

Sample No.	S1	S2	S3	S4	S5	S6
m value (CTF)	0.96	0.87	1.22	0.99	0.98	0.25
n value (IS)	0.30	0.41	0.49	0.30	0.29	0.59

Fig. 6: a) CTF variation with sample thickness and b) IS variation with sample thickness.

We propose the following formulas to relate the indentation indices to the sample thickness, T:

$CTF=aT^{m}$ and $IS=bT^{n}$ (3)

where m and n values were assessed from Fig. 6 and plotted against UCS (see Fig. 7). Using the Sigma Plot software, nonlinear regression curves in polynomial, inverse first order equations were then passed through the data points in Fig. 7 resulting in the following two correlations for m and n parameters:

m-value for CTF $m = 1.16 + (-27.67 / UCS)$ R=0.91(4)

n-value for IS $n = 0.31 + (8.27 / UCS)$ R=0.72(5)

In Eqs. (4) and (5), UCS is in MPa. Using the correlation equations in Fig. 6 and Eqs. (4) and (5), we propose the normalized indentation indices (CTF_n and IS_n) as follows:

$$CTF_n = \frac{CTF}{T^m} \quad (6)$$

$$IS_n = \frac{IS}{T^n} \quad (7)$$

where, T is ratio of fragment thickness to the unit thickness in terms of mm/mm. The conventional indentation indices were measured from the load-penetration curves and normalized through Eqs. (6) and (7). The normalized indentation indices were plotted to show the performance of the thickness function in reducing the size dependency of the conventional indices (Fig. 8).

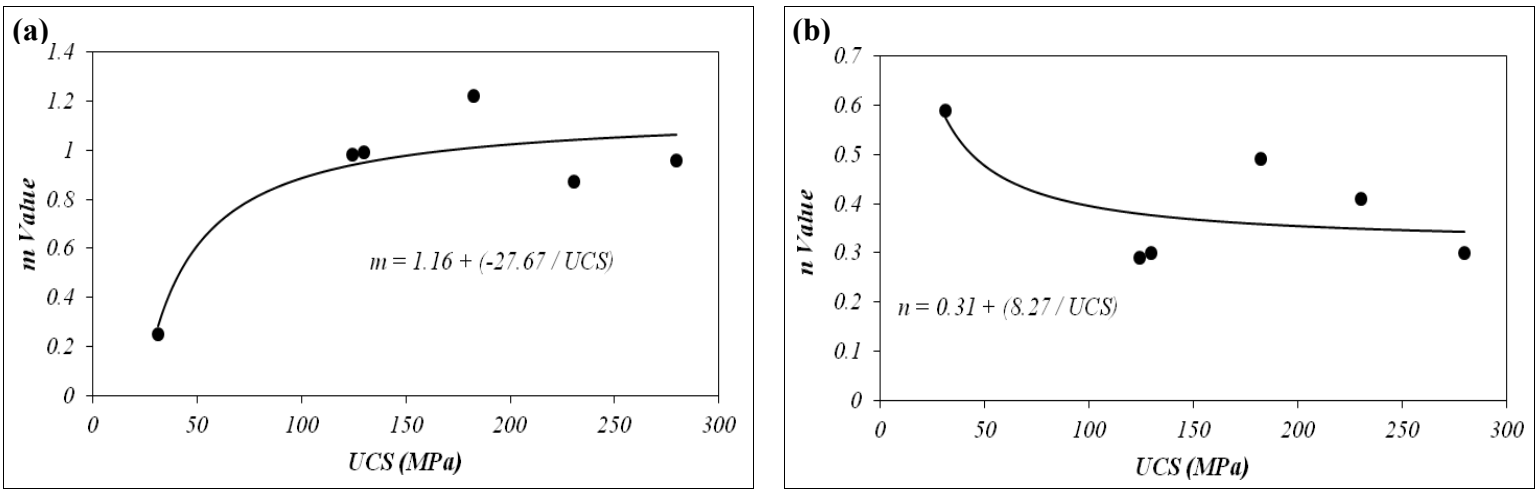

Fig. 7: a) m values against UCS for CTF and b) n values against UCS for IS.

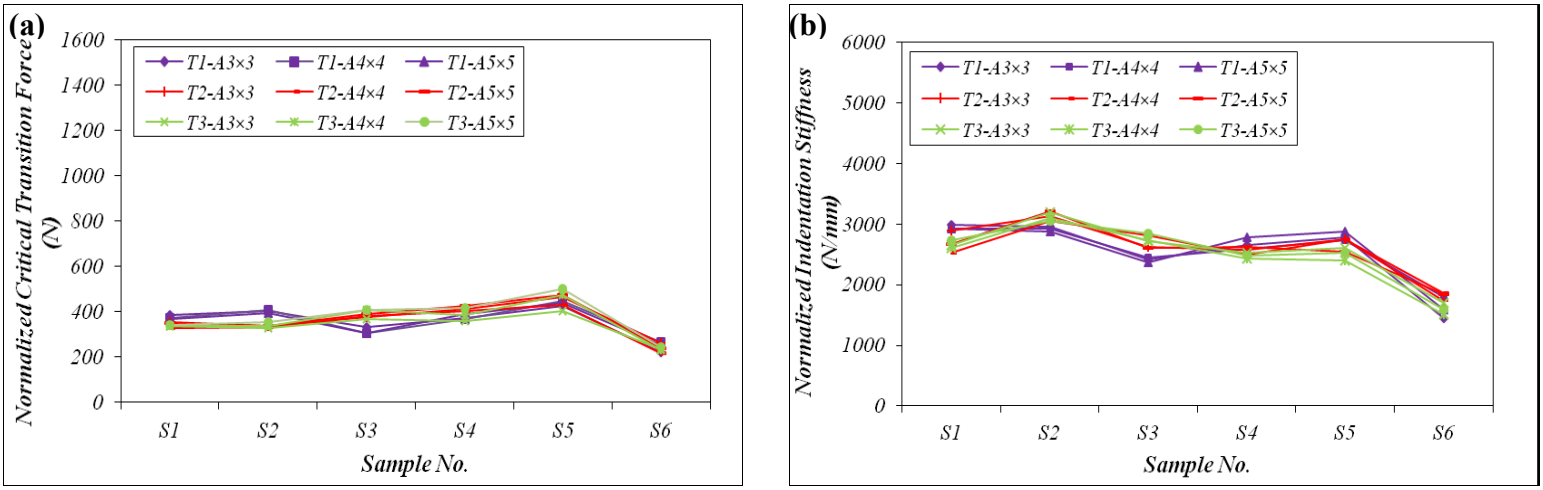

Fig. 8: a) Variation of normalized critical transition force with sample size and b) variation of normalized indentation stiffness with sample size.

Next, the normalized indentation indices were plotted against the core UCS and correlation curves were drawn for same-size samples, which resulted in correlation coefficients of greater than 0.60 for CTF_n and 0.85 for IS_n (Fig. 9). Nearly matching correlation curves in Fig. 9 suggests that the thickness functions can be used for effective normalization of indentation test results.

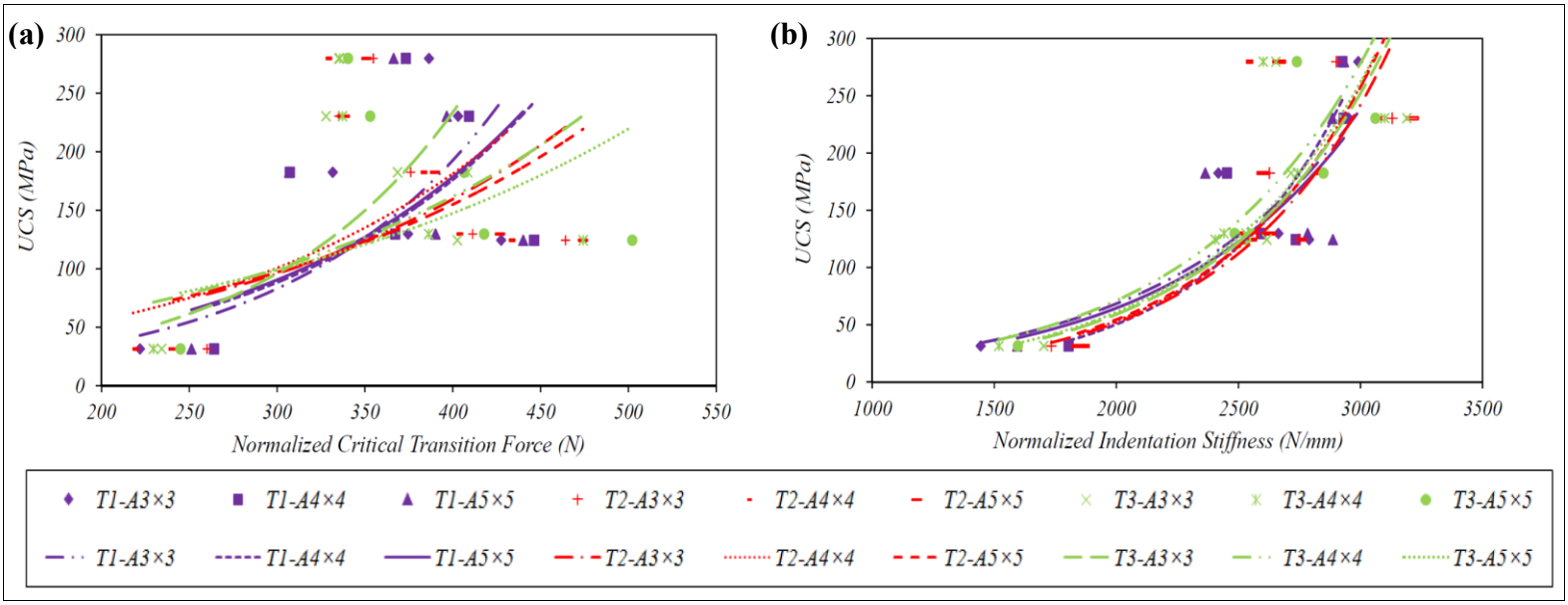

Fig. 9: Correlation curves of the normalized indentation indices and the corresponding UCS; a) normalized critical transition force and b) normalized indentation stiffness. Each curve is obtained from the correlating the UCS and the normalized indentation indices of the fragments with the same dimensions. (Legend is same in both a and b which is presented below the curves).

A linear relationship was tried between the normalized critical transition force and the normalized indentation stiffness which showed a correlation coefficient of 0.64. Fig. 10 plots the normalized indentation indices versus the corresponding core UCS. Using the exponential

regression, correlation coefficients are greater than 0.55 for CTF_n - UCS correlation and equal to 0.90 for correlation between IS_n and UCS. From the relationship between the normalized indentation indices and UCS, the following correlation equations were obtained:

$$UCS = 17.19e^{0.0057\,(CTF\ n)} \qquad R = 0.55 \qquad (8)$$

$$UCS = 3.48e^{0.0014\,(ISn)} \qquad R = 0.90 \qquad (9)$$

Substitution of Eqs. (4) through (7) in these correlation equations give:

$$UCS = 17.19\, e^{0.0057\left(\frac{CTF}{T^{1.16+\left(\frac{-27.67}{UCS_{assu.}}\right)}}\right)} \qquad (10)$$

$$UCS = 3.48\, e^{0.0014\left(\frac{IS}{T^{0.31+\left(\frac{8.27}{UCS_{assu.}}\right)}}\right)} \qquad (11)$$

To estimate UCS from Eqs. (10) and (11), an iterative progression should be done. First, a value for UCS is assumed and put into the right side of the equation (UCS_{assu}) to calculate UCS. Next, the calculated UCS is considered as the UCS_{assu} in the right side and is recalculated the equation. This sequence is continued until the assumed UCS (UCS_{assu}) and the calculated one become identical.

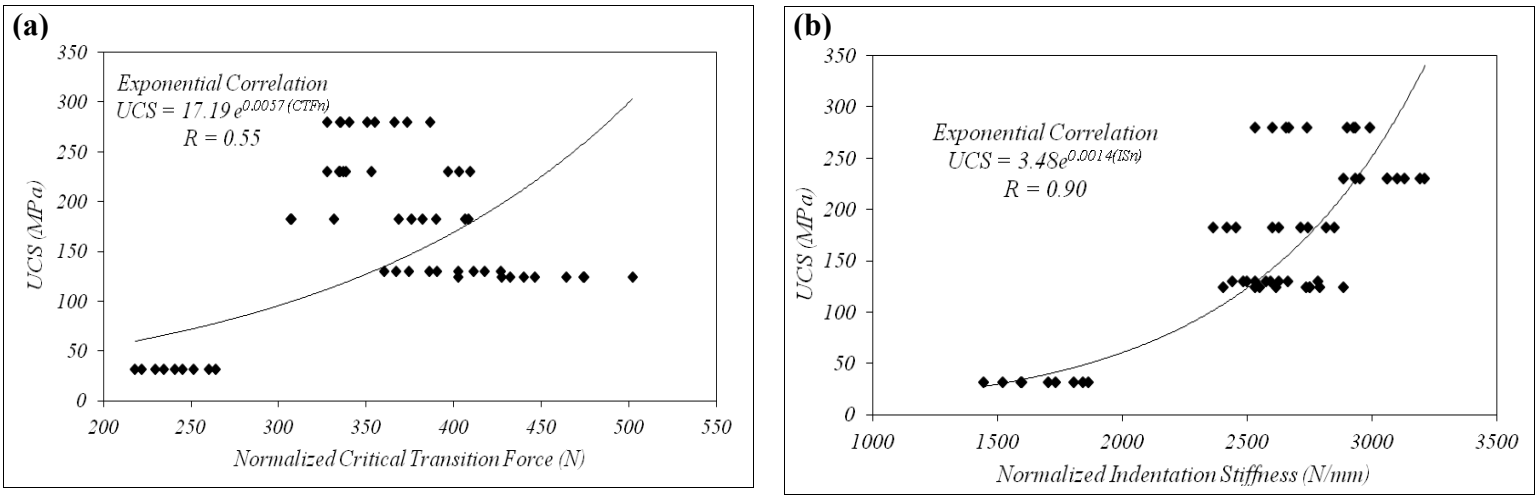

Fig. 10: Exponential regression of uniaxial compressive strength (UCS) with a) normalized critical transition force (CTF_n) and b) normalized indentation stiffness (IS_n).

4. Verification of the Correlations

To verify the correlations equations (10) and (11), the measured and predicted UCS for samples from blocks S7, S8 and S9 were compared. A total of 270 artificial rock fragments were produced and embedded in 27 epoxy-resin disks. Sample preparation and testing method were described in Section 2.

From the load-penetration curves, average IS and CTF values were determined. Average value of the coefficients of variation for IS and CTF were generally less than 10% for each of these sample groups.

The UCS of limestone blocks was predicted using the normalized indentation indices (IS_n and CTF_n) through the iterative progression of proposed correlations; Eqs. (10) and (11).

Fig. 11 shows the measured and estimated UCS for samples from blocks S7, S8 and S9 relative to the line X=Y. The estimated UCS are close to the measured UCS values when using IS_n, while they are more scattered when using CTF_n for estimation. The estimated UCS value from the IS_n correlation shows less scatter for weaker samples than the strong samples. In order to explore the details of these correlation equations and to provide better correlations, more experimental work is required. However, for further examination of the proposed correlations, the laboratory measured UCS of blocks S7, S8 and S9 and the normalized indentation indices were added to the data shown in Fig. 10, and are presented in

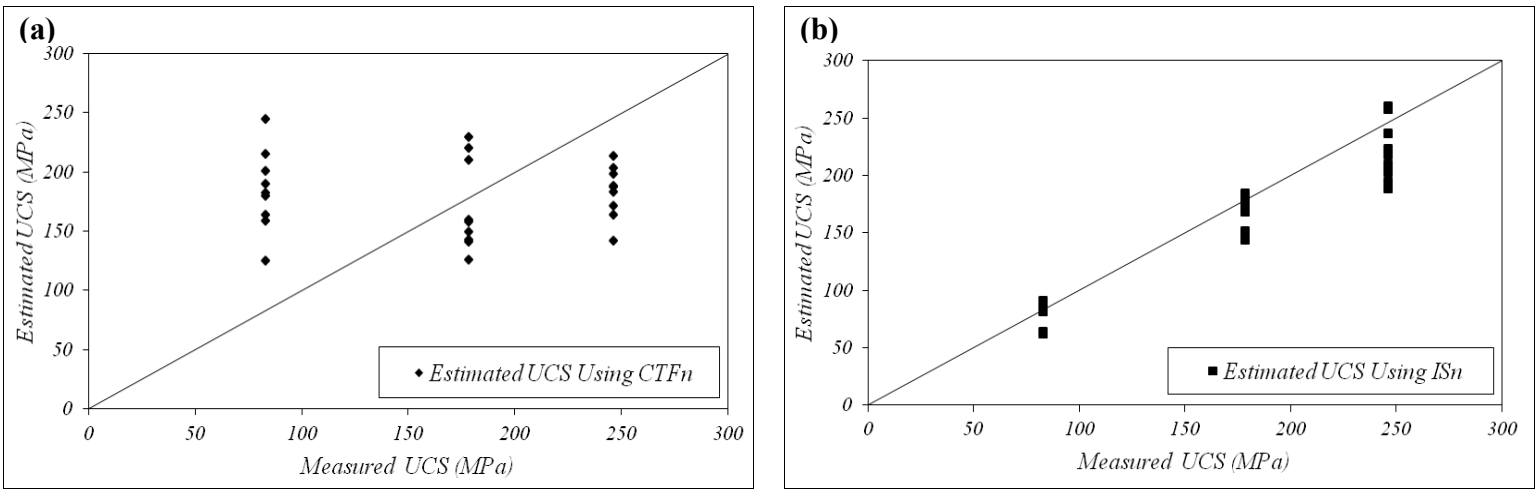

Fig. 11: Scatter of the predicted and measured UCS values using rock blocks S7, S8 and S9 to investigate their fitness to the linear relation.

Fig. 12 (the red-marked data points). The red points were reasonably close to the exponential correlation curve. The correlation is improved when using IS_n (Figs. 11b and 12b). Thus, both IS_n and CTF_n equations can be used to estimate the UCS of rocks from drill cuttings where no cores are available, but the UCS-IS_n correlation is preferred. Obviously, the

estimated value of UCS for the sample with UCS of about 80 MPa from correlation between CTF_n and UCS (Eq. 10) is quite large. However, this implies that using the CTF_n equation for estimating UCS may not be suitable.

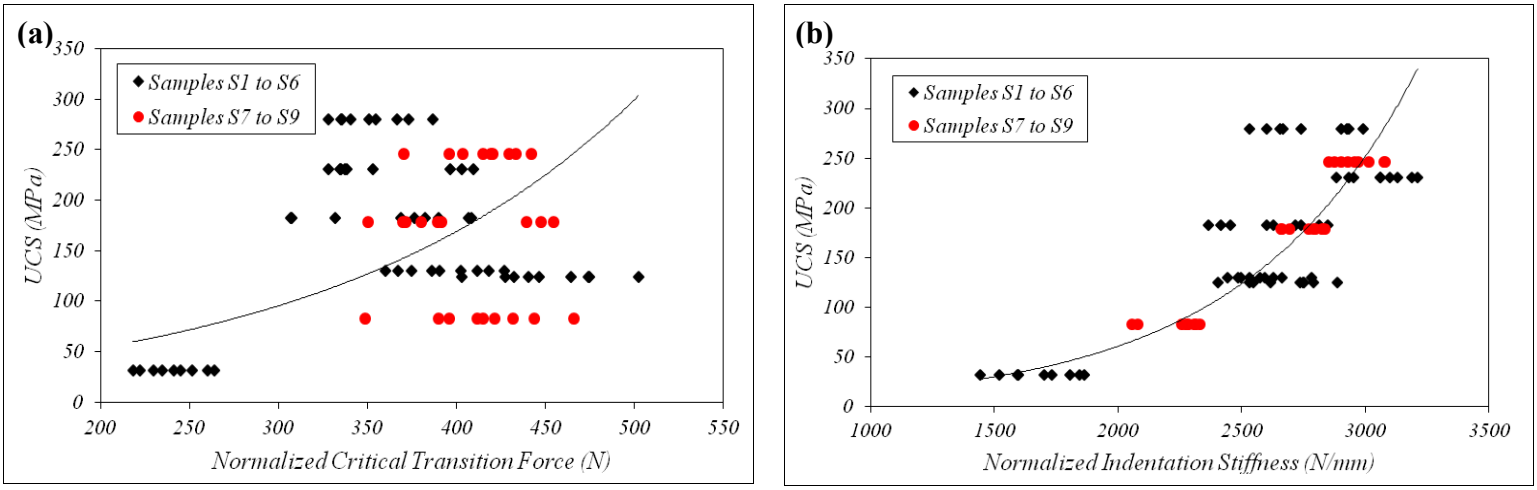

Fig. 12: Scatter of laboratory measured UCS values and normalized indentation indices pertinent to the blocks S7, S8 and S9 on the correlation curves of Fig. 10, (the black diamonds are samples S1 to S6 and the red circles are samples S7 to S9).

5. Conclusions

Laboratory indentation testing on rock fragments in the size range of drill cuttings (less than 5 mm) was used to predict the UCS and investigate size dependency of the indentation indices. Rock blocks were selected from various types of limestone collected from overburden rocks from Iranian oil fields. The UCS of rock cores was determined in laboratory. Small rock fragments were made in rectangular cuboid shape with cross sectional area of 3×3, 4×4 and 5×5 mm^2 and different thicknesses of 1, 2 and 3 mm.

The indentation test results are affected by sample thickness but are not sensitive to cross sectional area of fragments normal to loading direction. Thicker samples showed higher indentation indices. The indentation indices were normalized using a parameter which was a function of thickness and rock strength.

Average values of the normalized critical transition force (CTF_n) and normalized indentation stiffness (IS_n) were compared with the corresponding UCS values, which indicated correlation coefficients greater than 0.55 and 0.90, respectively. Correlation equations were proposed using the exponential regression to assess the intact rock UCS from the normalized indentation indices.

The proposed correlations were verified using the normalized indentation indices of independent limestone blocks. Results show that the estimated UCS values are reasonably

close to the measured ones in the laboratory. The reasonable correlation between indentation indices and the UCS of rock cores, verification results and the simplicity of the indentation testing indicate the potential of this technique in estimating UCS from drill cuttings at low operational cost. We would recommend using IS_n for estimating the UCS since it shows a higher correlation coefficient.

It should be noted that the proposed correlations are valid for the limestone rocks with rock fragment sizes between 3-5 mm using the same sample preparation method as described in this paper. Further investigations are required to study the indentation indices to refine the correlations by including data from other geographical locations and different lithologies as well as other parameters controlling the test results including indenter diameter and loading penetration rate.

References

[1] Bieniawski ZT. Rock mass classification in rock engineering, exploration for rock engineering. In: Proc. Symp., Cape Town. Balkema, Cape Town 1976; p. 97-106.

[2] Bieniawski ZT. Engineering rock mass classification. New York: Wiley; 1989.

[3] Ozkan I, O'zarslan A, Genis M, Ozsen H. Assessment of scale effects on uniaxial compressive strength in rock salt. Environmental & Engineering Geosciences 2009; 15:91-100.

[4] Okubo CH. Rock mass strength and slope stability of the Hilina slump, Kilauea volcano, Hawai'i. Journal of Volcanology and Geothermal Research 2004; 138:43-76.

[5] Gurocak Z, Alemdag S, Zaman MM. Rock slope stability and excavatability assessment of rocks at the Kapikaya dam site, Turkey. Engineering Geology. 2008; 96:17-27.

[6] Uboldi V, Civolani L, Zausa F. Rock strength measurements on cutting as input data for optimizing drill bit selection. In: SPE Annual Conference and Exhibition. Houston, Texas; 3-6 October 1999. SPE, ENI SpA 56441.

[7] Garcia RA, Saavedra NF, Calderón ZH, Mateus D. Development of experimental correlations between indentation parameters and unconfined compressive strength (UCS) values in shale samples. CT&F-Ciencia Tecnologíay Futuro. 2008; 3:61-81.

[8] Zausa F, Civolani L, Brignoli M, Santarelli FJ. Real time wellbore stability analysis at the rig site. In: SPE/IADC Drilling Conference. Amsterdam; 1997. SPE 37670.

[9] Germanovich LN, Dyskin AV. Fracture mechanisms and instability of openings in compression, Int. J. Rock Mech. Min. Sci. 2000; 37:263-284.

[10]Zhang L, Cao P, Radha KC. Evaluation of rock strength criteria for wellbore stability analysis. Int. J. Rock Mech. Min. Sci. 2010; 47:1304-1316.

[11]Yi X, Valko PP, Russell JE. Effect of rock strength criterion on the predicted onset of sand production. International Journal of Geomechanics. 2005; 5:66-73.

[12]ASTM, American Society for Testing and Materials. Standard test method for unconfined compressive strength of intact rock core specimens. ASTM D2938; 1984.

[13]ISRM, International Society of Rock Mechanics. Suggested methods for determining the uniaxial compressive strength and deformability of rock materials. Int. J. Rock Mech. Min. Sci. Geomech. Abs. 1979; 16:135-140.

[14]Fjær E. Static and dynamic module of weak sandstones. In: Rock mechanics for industry, B Amadei et al., editors. Rotterdam: Balkema 1999. pp. 675-81.

[15]Mateus J, Saavedra NF, Calderon ZH, Mateus D. Correlation development between indentation parameters and uniaxial compressive strength for Colombian sandstones. CT&F-Ciencia Tecnologíay Futuro. 2007; 3:125-135.

[16]Plumb R. Influence of composition and texture on the failure properties of clastic rocks. In: SPE/ISRM Proceedings of the Eurock'94. Rock mechanics in petroleum engineering, Rotterdam: Balkema 1994. pp. 13-20.

[17]Horsrud P. Estimating mechanical properties of shale from empirical correlations. In: SPE Drill Completion 2001. pp. 68-73.

[18]Tugrul A, Zarif IH. Correlation of mineralogical and textural characteristics with engineering properties of selected granitic rocks from Turkey. Engineering Geology 1999; 51:303-317.

[19]Kekec B, Unal M, Sensogut C. Effect of the textural properties of rocks on their crushing and grinding features. Journal of University of Science and Technology Beijing 2006; 13:385-389.

[20]Zorlu K, Gokceoglu C, Ocakoglu F, Nefeslioglu HA, Acikalin S. Prediction of uniaxial compressive strength of sandstones using petrography-based models. Engineering Geology 2008; 96:141-158.

[21]Santarelli FJ, Marshala AF, Brignoli M, Rossi E, Bona N. Formation evaluation from logging on cuttings. In: SPE Permian Basin Oil and Gas Recovery Conference, Midland, Texas; 27-29 March 1996; SPE 36851.

[22]Nes OM, Horsrud P, Sonstebo EF, Holt RM, Ese AM, Okland D, Kjorholt H. Rig-Site and laboratory use of CWT acoustic velocity measurements on cuttings. Paper SPE 36854 presented in the 1996 SPE European Petroleum Conference, Milan, Italy 1998.

[23] Mehrabi Mazidi S, Haftani M, Bohloli B, Cheshomi A. Measurement of uniaxial compressive strength of rocks using reconstructed cores from rock cuttings. Journal of Petroleum Science and Engineering. 2012; 86-87:39-43.

[24] Ringstad C, Lofthus EB, Sonstebo EF, Fjær E, Zausa F, Fuh GF. Prediction of rock parameters from micro-indentation measurements: the effect of sample size. In: EUROCK '98, Trondheim, Norway, 8-10 July 1998. SPE 47313.

[25] Zausa F, Santarelli FJ. A new method to determine rock strength from an index test on fragments of very small dimension. In: VIII ISRM International Congress on Rock Mechanics, Tokyo, Japan, 1995.

[26] Szwedzicki T. Technical note on indentation hardness testing on rock. Int. J. Rock Mech. Min. Sci. 1998; 35:825-829.

[27] Flügel E. Microfacies of Carbonate Rocks: Analysis, Interpretation and Application, Springer, 2004. ISBN 978-3-540-22016-9.

[28] Gill DE, Corthesy R, Leite MH. Determining the minimal number of specimens for laboratory testing of rock properties. Engineering Geology. 2005; 78:29-51.